SIMULATION TEST AND VERIFICATION OF MATERIAL CONVEYING FOR SMALL AND MEDIUM-SIZED AIR SUCTION JUJUBE PICKING MACHINE BASED ON CFD-DEM COUPLING

/

基于CFD-DEM 耦合中小型气吸红枣捡拾机物料输送仿真试验与验证

Fengkui ZHANG[1,2,3], Wenxi SHAO[1)], Shijie ZHAO[1,2,3)], Jikui ZHU[1,2,3)], Ping LI [1,2,3*]

[1)] College of Mechanical and Electrical Engineering, Tarim University, Alar 843300, Xinjiang, China;

[2)] Modern Agricultural Engineering Key Laboratory at Universities of Education Department of Xinjiang Uygur Autonomous Region, Tarim University, Alar 843300, Xinjiang, China

[3)] Key Laboratory of Tarim Oasis Agriculture (Tarim University), Ministry of Education, Tarim University, Alar 843300, Xinjiang, China

**Corresponding Author: Li Ping, Email: lpdyy716@163.com*

DOI: https://doi.org/10.35633/inmateh-71-46

Keywords: *Jujubes, Transportation, CFD-DEM coupling, Numerical simulation*

ABSTRACT

To improve the quality of air suction jujube picker, the CFD-DEM coupled method is used to numerically simulate the conveying process of jujube particles and explore the motion state, particle collision and energy loss of jujube particles in the pipeline. The erosion rate is selected as an evaluation index to discuss the influence of wind velocity, bending angle and diameter on the conveying process. The simulation results show that the collisions between jujubes, as well as the collisions between jujubes and pipe wall have an impact on the conveying performance, and the latter is more significant. The erosion rate is positively correlated with the wind velocity, negatively correlated with the pipe diameter, and the bending angle first decreases and then increases. The influence degree of factors on the erosion rate is: wind velocity > bending angle > pipeline diameter. The optimal parameter combination is a wind velocity of 28 m·s-1, a bending angle of 105 °, and a pipe diameter of 130 mm. At this time, the value of erosion rate is the lowest and the number of collisions and energy loss between jujube particles are reduced by 37.3 % and 13.87 % year-on-year, and those between jujube particles and pipe wall are reduced by 17.45 % and 17.61 % year-on-year, respectively. The test results show that the conveying pipe with optimized structural parameters can reduce the jujube skin damage rate by 2.06 %. The results of this study can provide a reference for the design and optimization of the air suction jujube picker.

摘要

中小型气吸式红枣捡拾机利用负压吸送原理完成红枣果实的输送作业，但因红枣与红枣、红枣与管壁碰撞等问题造成红枣表皮轻微损伤，为提高气吸式红枣捡拾机作业质量，利用 CFD-DEM 耦合的方法对输送管输送红枣颗粒过程进行数值模拟，探究红枣颗粒在管路内的运动状态、颗粒碰撞及能量损失情况，并以侵蚀速率为评价指标讨论风速、弯管角度和直径对输送过程的影响。仿真结果表明，红枣与红枣、红枣与管壁两种碰撞均对输送性能有影响，且后者更为显著；侵蚀速率与风速呈正相关，与管路直径呈负相关，与弯管角度则呈现先减小后增大；各因素对侵蚀速率的影响程度为风速>弯管角度>管路直径，最优参数组合为风速 28m•s-1，弯管角度 105°，管路直径 130mm，此时侵蚀速率值最低且枣间颗粒碰撞次数和能量损失同比降低 37.3%和 13.87%，红枣颗粒与管壁碰撞次数和能量损失同比降低 17.45%和 17.61%。验证试验结果表明，结构参数优化后的输送管对红枣表皮损伤率降低 2.06%。该研究结果可为气吸式红枣捡拾机的设计与优化提供参考。

INTRODUCTION

The research on mechanized harvesting equipment of jujubes mainly focuses on small and medium-sized air suction jujube picker *(Yuan et al., 2021; Yuan et al., 2022; Zhang et al., 2019)*. Its main function is to complete the tasks such as picking and conveying *(Zhang et al., 2020; Zhang et al., 2021)*, and separating and removing impurities of jujubes lying on the ground *(Du et al., 2022; Shi et al., 2022a)*. Because its selling price meets the cost demand of fruit farmers for harvesting, it is widely used in southern Xinjiang region, such as Kashgar, Aksu, Hotan and other places.

Fengkui Zhang, Master, Lecturer; Wenxi Shao, Graduate student; Shijie Zhao, Graduate student; Jikui Zhu, Lecturer; Ping Li, PhD, Professor.

The conveying process of small and medium-sized air suction jujube picker is mainly through the conveying pipeline of the picking device. In its negative pressure suction conveying process, the main flow is gas-solid two-phase. In actual production, it is found that the structure of conveying pipeline has a significant impact on the quality of the whole machine, especially on the jujube skin caused by a slight damage, which is not conductive to preservation and sale.

The discrete element method *(Basu et al., 2021; Jayasundara et al., 2022; Brandt et al., 2023; Carr et al., 2023)* and computational fluid dynamics numerical simulation techniques *(Nijssen et al., 2023; Rakesh and Shibayan, 2023; Weaver et al., 2023)* have become important tools for studying multiphase flow and structural optimization. The experimental method based on Computational Fluid Dynamics-Discrete Element Method (CFD-EDM) coupling is widely used to study the motion state between particles, as well as between particles and shells, and the characteristics in the airflow field *(Lewis et al., 2022; Ponzini et al., 2021; Hesse et al., 2023; Dustin et al., 2023)*. The method has also been used in the field of agricultural engineering to study the state of particles in the shell under the action of airflow, as well as to optimize the operation and structural parameters of key devices *(Leno et al., 2023; Kim et al., 2019; Qin et al., 2023)*. After optimization, the quality of mechanical equipment can be improved, such as small nut harvesting, grain sorting and seeder, et al. *(Ren et al., 2023; El-Emam et al., 2021; Hou et al., 2023)*.

The objectives of this study are: (1) the CFD-DEM coupling method is used to numerically simulate the conveying process of jujube particles in the conveying pipe of the small and medium-sized air suction jujube picking machine, so as to obtain the motion characteristics of jujube particles during the conveying process, the characteristics of airflow field distribution, as well as the relationship between the number of collisions and energy loss and the structural parameters of the conveying pipe; (2) through analyzing the movement state of jujubes in the conveying process, the distribution law in airflow field and the relationship between the collision and energy loss and the structural parameters of the conveying pipe is analyzed, and the optimization scheme of the conveying pipe structure is proposed; (3) the feasibility of the simulation results are verified, aiming to provide a reference for the design and optimization of small and medium-sized air suction jujube picking machine.

MATERIALS AND METHODS

Structure and Working Principle of the Picking Device

The picking device of the small and medium-sized air suction jujube picking machine (Fig. 1) includes a conveying pipe, separation and impurity removal box, unloading device and centrifugal fan and other more. Its working principle is to generate negative pressure inside the separation and impurity removal box through the centrifugal fan. Due to the pressure difference, the external airflow enters the mouth of the conveying pipe, and then the jujubes are picked and conveyed to the separation and debris removal box. The separation of materials and impurities, as well as the collection of materials, can be achieved through the separation and removal box and discharge device.

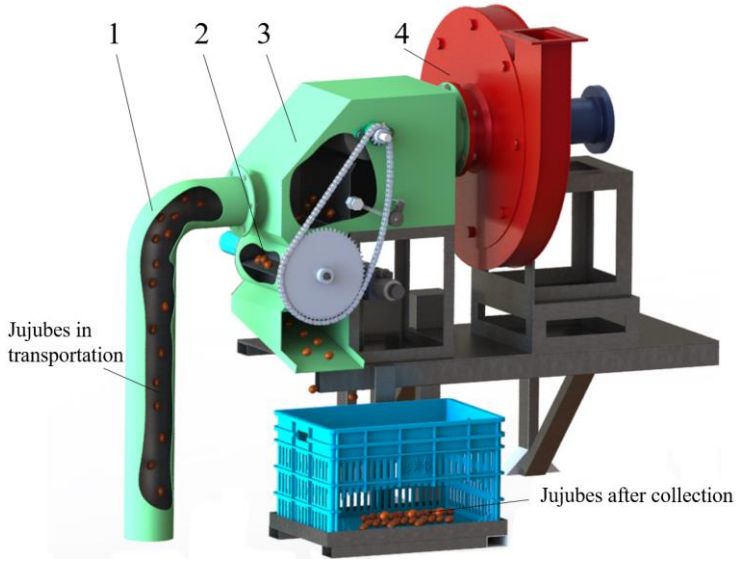

Fig. 1 - Picking device

1. Conveying pipe; 2. Unloading device; 3. Separation and debris removal box; 4. Centrifugal fan

A conveying pipe usually consists of a section of 90° metal elbow and a PU corrugated ventilation pipe with the same inner diameter as the outer diameter of the elbow connected through a stain less steel throat hoop. The flange plate welded at the outlet of the metal elbow can be connected to the flange bolt at the inlet of the separation and impurity removal box, ensuring that the working quality of the suction jujube picker cannot be reduced due to air tightness during the conveying process. According to the requirements of coupled numerical simulations, the grid size needs to be slightly larger than the material size. The cell grid size of the ANSYS Wrokbench in the ICEM module is set to 30 mm, and the pipeline is divided into grids using the swept method. The grid is quadrilateral, with a vertical section height of 700 mm, a horizontal section length of 200 mm, an elbow diameter of 130 mm, and a total number of grids of 2544. Its minimum cell mass, maximum cell mass and average mass are 0.618, 0.977 and 0.875, respectively. The grid quality meets the simulation requirements. After setting, the divided grid is shown in Fig. 2

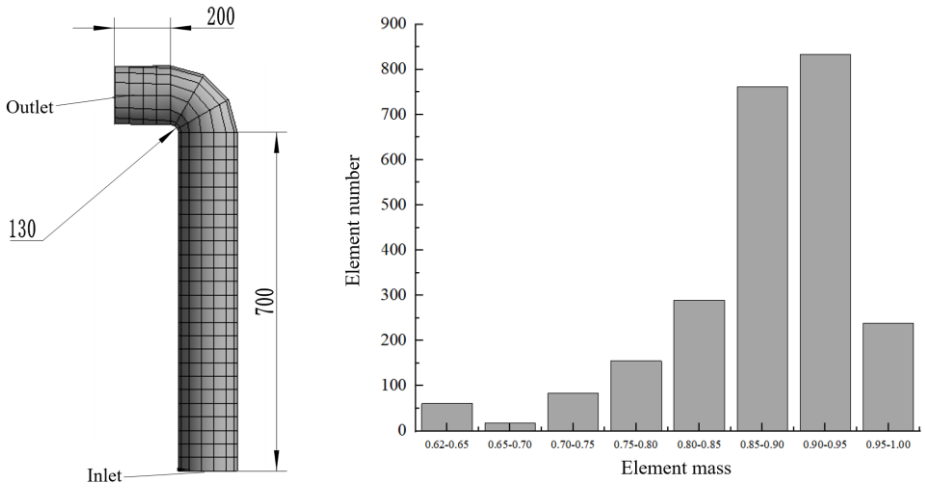

Fig. 2 – Grids of the conveying pipe

CFD-DEM coupled model construction

Fluent fluid model

Due to the high airflow velocity (which is generally greater than the suspension velocity of jujubes) during the transportation of jujube particles in the fluid, the void rate between jujubes is large, which belongs to the rarefied-phase pneumatic conveying. The Eulerian coupling model is used in the coupling, and the Wen & Yu model selected the traction model, which has the characteristics of adapting to large void rate and more meets the actual situation of jujube particle transportation process.

The Eulerian coupling model is used to simulate the transportation process of jujube particles, and the fluid volume fraction term and the differential equation of fluid motion are expressed as follows *(Weng et al., 2022)*:

$$\frac{\partial_{\varepsilon\rho}}{\partial_t}+\nabla(\rho\varepsilon\mu)=0 \tag{1}$$

$$\frac{\partial_{\varepsilon\rho}}{\partial_t}+\nabla(\rho\varepsilon\mu v)=-\nabla P+\nabla(\rho\varepsilon\nabla v)+\rho\varepsilon g-S \tag{2}$$

where t is the time; ε is the fluid volume fraction term; v is the flow velocity; g is the gravitational acceleration; ρ is the fluid density; S is the momentum source term; μ is the coefficient of viscosity; P is the pressure on the fluid microelement, and ∇ is the Hamiltonian differential operator.

The momentum source term S is the sum of the airflow resistance of the airflow acting inside the cell grid *(Hu et al., 2020)*.

$$S=\frac{\sum_{i=1}^{n}F_i}{V} \tag{3}$$

where V is the cell grid volume, and F_i is the resistance of the i-th particle to the airflow.

DEM solid particle contact and collision model

The contact mechanical behavior and interaction force between particle mechanical models are simulated and analyzed in EDEM software.

Since the velocity between the particles changes with the contact force, the jujubes are mainly subject

to rolling friction and air flow in the gas-solid two-phase flow, with no adhesion on the surface of jujubes. The Hertz-Mindlin no-slip contact model and the soft-sphere dry contact model are selected *(Wiacek, 2016)*, and the motion equations of the *i*-th particle are obtained according to Newton's second law *(Hamed et al., 2023)*:

$$m_i \frac{dV_i}{d_t} = m_i g + P = \sum_{j=1}^{n_i} \left(F_{n,ij} + F_{t,ij} \right) \quad (4)$$

$$I_i \frac{d\omega_i}{d_t} = \sum_{j=1}^{n_i} \left(T_{n,ij} + T_{t,ij} \right) \quad (5)$$

where g is the gravitational acceleration; P is the interaction force on the particles when they move in the airflow; I_i and m_i are the rotational moment of inertia and mass of particle i, respectively; V_i and ω_i are the velocity and angular velocity of particle i, respectively; $F_{t,ij}$ is the tangential component force; $F_{n,ij}$ is the normal component force; $T_{r,ij}$ is the rolling friction torque, and $T_{t,ij}$ is the tangential force torque.

According to the linear three-equation functional model of elastic damping, each force is simplified in the form of a combination of spring, damping, and slider form *(Xiong et al., 2019)*:

$$F_{n,ij} = -k_n \delta_n - n_n V_{n,ij} \quad (6)$$

$$F_{t,ij} = -k_t \delta_t - n_n V_{n,ij} - \frac{f_s |F_{n,ij}| \delta_t}{|\delta_t|} \quad (7)$$

$$T_{t,ij} = L_{ij} n_{ij} \times F_{t,ij} \quad (8)$$

$$F_{r,ij} = -k_r a - n_r \omega_{ij} - \frac{f_r |F_{n,ij}| a}{|a|} \quad (9)$$

where V is the velocity of motion of particles; δ is the displacement deformation between particles; a is the torsional deformation; k is the stiffness coefficient; f is the friction coefficient; η is the damping coefficient, and L is the amount of overlap. ij is between particles i and particles j, t is tangential, n is normal, s is sliding, and r is circumferential or rolling.

The interaction force P that particles are subjected to in the gas stream is expressed as follows:

$$P = k_g \rho A v^2 = k_g \rho A (v_q - v_w)^2 \quad (10)$$

where ρ is the density of the airflow; k_g is the drag coefficient, which is related to the shape of the material structure, surface characteristics and Reynolds number, etc. A is the area of the material facing the wind; v_w is the velocity of the material; v is the relative velocity of the material in the airflow; and v_q is the velocity of the airflow.

As shown in Table 1, the average equivalent diameter of jujube is 26.23 mm, and the particles are simplified to equivalent sphere. 26mm sphere particles are taken as the model of jujube particles, as shown in Fig. 3.

Table 1

Basic material parameters of jujube particles

Parameters	Work unit	Maximum values	Minimum value	Average value
Mass	g	8.12	2.91	4.87
Volumetric	ml	14	6	9.46
Densities	g·cm^{-3}	0.604	0.473	0.534
Equivalent diameter	mm	29.89	22.53	26.23

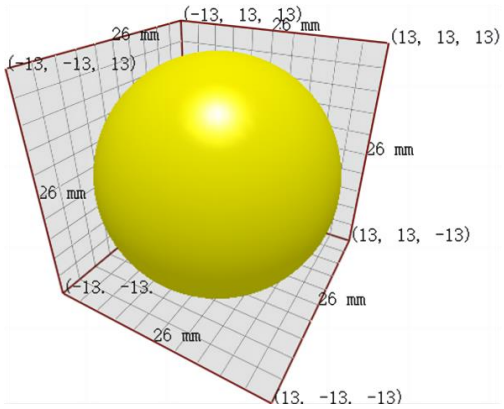

Fig. 3 - Jujube particle model

Performance evaluation index selection for CFD-DEM coupled conveying process

In response to the current simulation state of jujube conveying process in the conveying pipe, the erosion rate is taken as an evaluation index. Its principle is to simulate the erosion corrosion caused by particles in the fluid on the inner wall of the pipeline. The erosion rate is affected by wind velocity, pipe diameter, bending angle and other factors. To explore the effects of wind velocity, pipe diameter, bending angle and other factors on the conveying process, the control variables method is used to ensure that the other conditions have the same parameters in the simulation of jujube conveying process. Taking the erosion rate as an index, the influence of each factor on the erosion of the pipeline is determined. The orthogonal test method is used to further study the influence of factor interaction on the performance of jujube conveying process.

The main measurement index for the working performance of the conveying pipe of the picking device of the air suction jujube picker is the jujube skin damage rate *E*. *E* is thus selected as the evaluation index of the working performance for the optimization and verification of the conveying pipe.

$$E=\frac{M_1}{M}\times 100\% \quad (11)$$

where M_1 is the number of jujubes that pass through the outlet with damaged epidermis during the verification test and *M* is the total number of exported jujubes during the verification test.

Numerical simulation parameterization

The mass, volume and density of jujube particles are measured by balance and cylinder method. The frictional contact parameters between jujubes and pipe wall are measured by the inclined plate test. The recovery coefficient between jujubes and pipe wall is measured by the collision method *(Zhang et al., 2018)*. The relevant parameters are obtained through the pre-test of relevant material parameters and relevant literatures as shown in Table 2 *(Shi et al., 2022b; Wang et al., 2021)*.

EDEM parameter settings

The specific parameters of the materials used in EDEM are shown in Table 2. The particle radius is random, with a range of 0.85 to 1.15. 200 particles are generated per second, with an initial velocity of 0.5 m·s^{-1}. The simulation time step is 1e-05 s, and storage is performed every 0.01 s.

Table 2

Related parameters and contact coefficients of particles and materials

Parameters	Items	Numerical values
Jujube particles	Poisson ratio	0.248
	Shear modulus (MPa)	0.06
	Densities (kg·m^{-3})	534
Pipeline	Poisson's ratio	0.319
	Shear modulus (MPa)	1139
	Density (kg·m^{-3})	1380
Particles - pipe wall	Crash recovery factor	0.75
	Coefficient of static friction	0.25
	Coefficient of rolling friction	0.03
Particles	Crash recovery factor	0.77
	Coefficient of static friction	0.48
	Coefficient of rolling friction	0.04

Fluent parameter settings

The Realizable k-ε model, no relative slip pipe wall, is adopted. The air is a fluid medium, with an inlet wind velocity of 28 m·s^{-1}, a turbulence intensity of 5% and a return intensity of 2.5% in Fluent. The control equations adopt Couple pressure equations, and the momentum term, turbulent kinetic energy and dissipation rate are all in second-order windward format. The residuals are set to 1e-06; the time step is 0.01 and the number of steps is 300.

RESULTS AND DISCUSSION

Dynamic Pressure, Airflow Velocity Distribution and Particle Motion in the Conveying Pipe

During the simulation, the particle plant is added at the inlet of the pipeline, and the number of particles generated per second is 200 for a total of 3 s. Fig. 4 (a) and (b) show the movement of particles in the elbow pipe at t=1.5 s.

It can be seen that the gas pressure in the horizontal and vertical sections of the pipeline is negative. The pressure from the outlet to the inlet of the material increases gradually, and the velocity of the gas in the pipe at this time is stable in 20.5-32.8 m·s^{-1}.

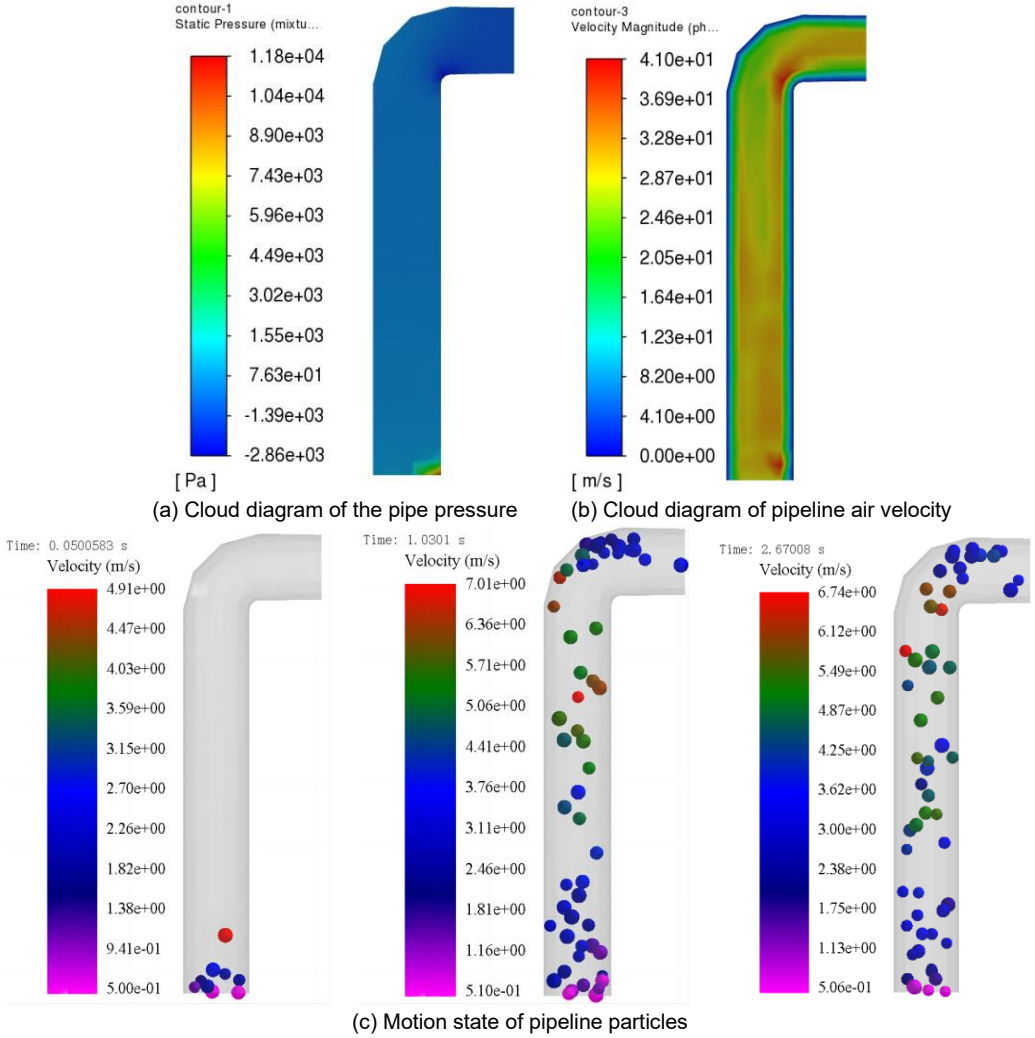

(a) Cloud diagram of the pipe pressure (b) Cloud diagram of pipeline air velocity

(c) Motion state of pipeline particles

Fig. 4 - Dynamic pressure, airflow velocity and particle motion in the conveying pipe

Fig. 4 (c) shows that jujube particles enters into the pipeline from the inlet, with an initial particle velocity of 0.5 m/s. Particles enter into an accelerated state through the vertical airflow, with most particles having a velocity of 3~4 m·s^{-1}, and a maximum velocity of 6~7 m·s^{-1}. In this stage, the closer the particle position, the faster the acceleration. The particles entering the elbow pipe are subjected to centrifugal force and collide with the outer wall of the elbow pipe, resulting in accumulation of jujube particles in the upper part of the elbow pipe and the phenomenon of particle bundles. In this stage, the particle velocity drops sharply to 2.41-3.71 m·s^{-1}. Subsequently, jujube particles enter the horizontal section under the pressure of the pipeline. In the horizontal section, the slightly larger jujube particles are located near the bottom of the horizontal pipeline in their own gravity, and small particles are mostly located above the large particles. According to the analysis of the overall motion state of particles, it can be seen that the distribution of particles in the three regions of the subsection are high on axis surrounded by low and granular bundles, and layered distribution, respectively.

Date particle collision and energy loss

There are two situations where jujube particles collide under the centrifugal force of airflow and pipeline: collisions between jujubes, and collisions between jujube particles and pipeline. Energy loss will occur as the collision at the same time. This energy loss will reduce the velocity of jujube particles, increase the energy consumption in the air suction conveying process, and is not conducive to jujube conveying. As shown in Fig. 5, the collision of jujube particles in the vertical section is less. After 0.3 s, there is a large amount of particle accumulation at the elbow, and the particle collisions and energy loss also increase accordingly. In this stage, the number of collisions per 0.2 s is about 104 times, with an average energy loss of 1.06 J.

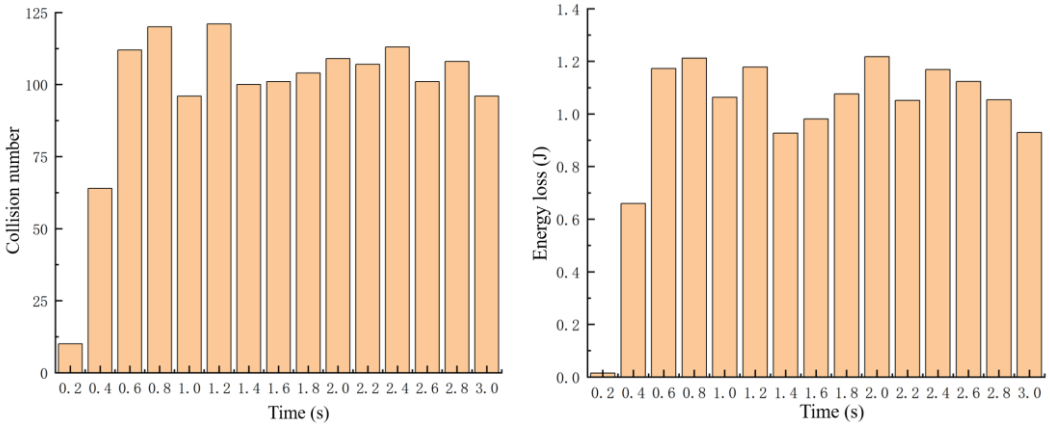

(a) Number of particle collisions between jujubes (b) Energy loss of particle collision between jujubes

Fig. 5 - Number of collisions and energy loss between jujubes

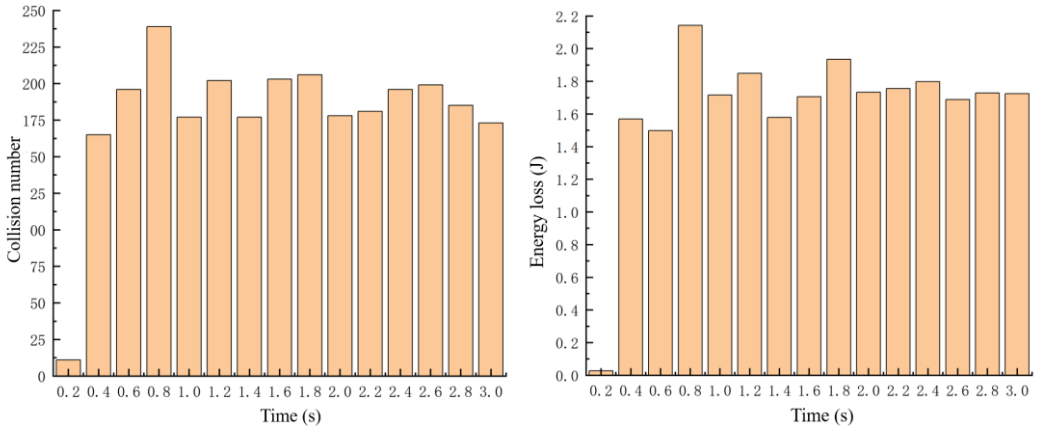

(a) Number of collisions between jujube particles and pipeline (b) Energy loss between jujube particles and pipe

Fig. 6 - Number of collisions and energy loss between jujube particles and pipe

It can be seen from the number of collisions and energy loss between particles and pipeline (Fig. 6) that, the collisions between the jujube particles and pipeline also occur mostly at the elbow, about 191 times, and the energy loss is 1.74 J.

According to the particle collision and energy loss during the overall movement of particles, it can be seen that the number of collisions between particles, as well as between particles and pipeline before the simulation time of 0.2 s are less. This is due to the scattered initial distribution of the material in the vertical section, with fewer particles in contact with each other and the pipeline. The majority of particles accumulate at the elbow, resulting in a large number of collisions and energy losses. Through data comparison, it can be found that there are certain differences in energy loss and collision frequency in each statistical interval. The number of collisions between particles and pipeline is 1.84 times that between particles, and the energy loss is 1.64 times. Therefore, the collision between jujube particles and the collision between jujube particles and pipeline particles simultaneously affect the conveying performance of jujubes. Particularly, the collision between jujube particles and pipeline has a more significant effect on the conveying performance.

Effect of wind velocity, bending angle and pipe diameter on erosion rate

Effect of wind velocity on erosion rate

The control variable method is used to explore the impact of different wind velocities on the erosion rate of the pipeline, and the test results are shown in Table 3. The test selects the wind velocities of 23, 28, 33, 38, and 43 $m \cdot s^{-1}$, a diameter of the elbow pipe of 130 mm, and a bending angle of 90° to simulate the erosion rate. The erosion efficiency under the five groups of wind velocities are 2.17e-7 $kg \cdot m^{-2} \cdot s^{-1}$, 3.62e-7 $kg \cdot m^{-2} \cdot s^{-1}$, 5.54e-7 $kg \cdot m^{-2} \cdot s^{-1}$, 7.8 4e-7 $kg \cdot m^{-2} \cdot s^{-1}$, and 1.03e-6 kg·m-2·$s^{-1}$, respectively.

Table 3

Pipe erosion rates under different wind velocities

Clusters	Wind velocity / m·s^{-1}	Erosion rates / kg·m^{-2}·s^{-1}
1	23	0.000000217
2	28	0.000000362
3	33	0.000000554
4	38	0.000000784
5	43	0.000001030

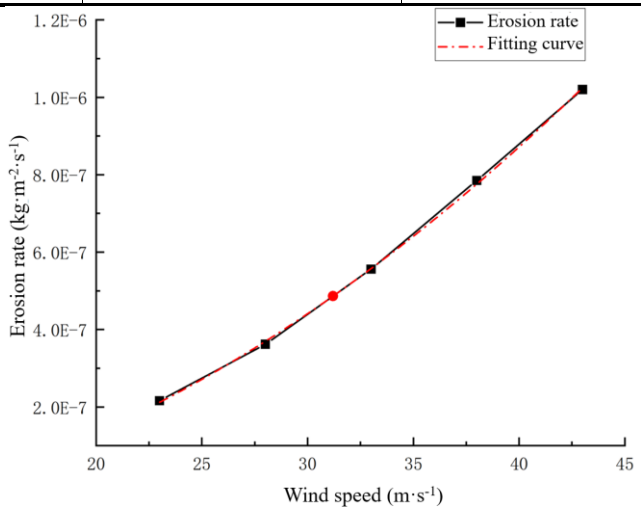

Fig. 7 - Relationship curve between the inlet wind velocity and the erosion rate

The relationship between the wind velocity and erosion rate of the pipeline is shown in Fig. 7, and its fitting curve function is: y = 6.09 e -10*x2+4.54 e-10*x-1.2e-7(R2=0.99957). It can be seen from Fig. 7 that the erosion rate increases linearly as the wind velocity increases. The increase of erosion rate is lower than 2e-7 in the interval of 23-38 m·s^{-1}, and that higher than 2e-7 in the interval of 43 m·s^{-1} or above.

Effect of bending angle on erosion rate

To investigate the effect of different bending angles on the erosion rate, only the bending angle is changed for a single factor test. Its wind velocity is 28 m·s^{-1}; the pipe diameter is 120 mm, and the bending angles are 90°, 97.5°, 105°, 112.5° and 120°, respectively. The test results are shown in Table 4.

Table 4

Erosion rates at different piping angles

Clusters	Bending angle (°)	Erosion rates / kg·m^{-2}·s^{-1}
1	90	0.000000373
2	97.5	0.000000369
3	105	0.000000362
4	112.5	0.000000365
5	120	0.000000372

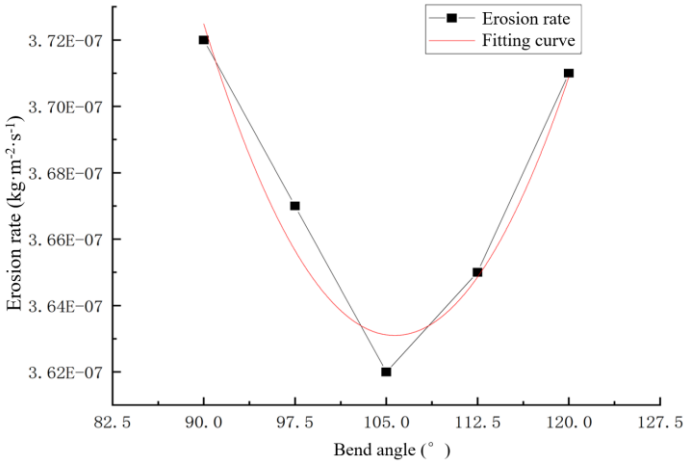

Fig. 8 - Relationship curve between the bending angle and erosion rate

The relationship between the bending angle and the erosion rate is shown in Fig. 8, and its fitting curve function is: y =3.81e-11*x2-8.05e-9*x+7.89e-7 (R2= 0.95211). The effect of the bending angle on the erosion rate of the law is that when the angle is in the range of 90-105°, the erosion rate continues to decrease and drops to the lowest point at 105 °, and then increases. Based on the experimental data and actual working conditions, 97.5-112.5° is selected as the reference factor range for orthogonal test.

Effect of the pipe diameter on the erosion rate

To determine the effect of the pipeline diameter on the erosion rate, the wind velocity is selected as 28 $m \cdot s^{-1}$, the bending angle as 90 °, and the diameters of the pipeline as 100 mm, 110 mm, 120 mm, 130 mm, and 140 mm, respectively. Three tests are carried out for each group, and the obtained data is shown in Table 5.

Table 5

Erosion rates at different bend diameters

Clusters	Pipe Diameter / mm	Erosion rates / $kg \cdot m^{-2} \cdot s^{-1}$
1	100	0.000000573
2	110	0.000000432
3	120	0.000000362
4	130	0.000000325
5	140	0.000000310

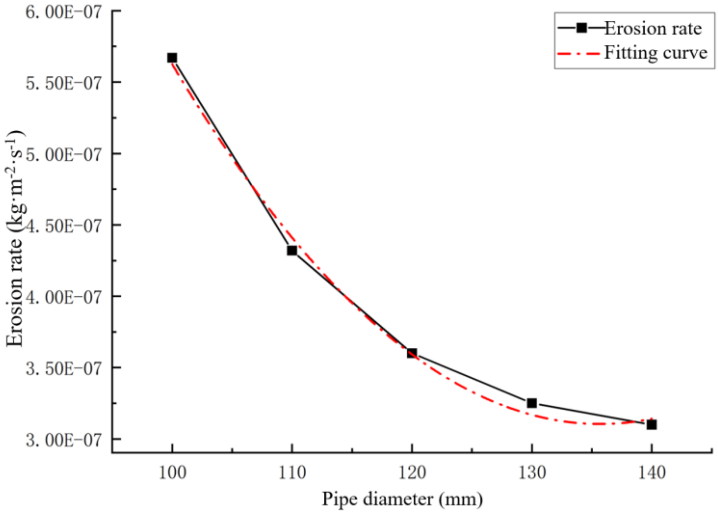

Fig. 9 - Relationship curve between the elbow diameter and the erosion rate

The relationship curve between the pipe diameter and the erosion rate is shown in Fig. 9. It shows that the erosion rate decreases as the pipe diameter increases. The decrease is large when the pipe diameter is in the range of 100-120 mm, and gradually reduced after 120 mm. It can be seen that the pipe diameter in the range of 120 -140 mm is more appropriate. A quadratic polynomial is used for fitting, and the fitted curve function is: y= -5.36957e -8*x2+1.97857e-10*x+ 3.95357e-6 (R2=0.99579).

Optimization simulation and analysis of the pipeline structural parameters

Determination of test factor levels

According to the test results of the wind velocity, bending angle, pipe diameter on the erosion rate, the wind velocity and erosion rate is positively correlated. Since the suspension velocity of jujubes needs to be greater than 28 $m \cdot s^{-1}$, 28~38 $m \cdot s^{-1}$ is selected as the factor level range of the orthogonal test according to the actual working conditions. Three levels: 28 $m \cdot s^{-1}$, 33 $m \cdot s^{-1}$, and 38 $m \cdot s^{-1}$ are selected. The bending angle and erosion rate first decrease and then increase, and the erosion rate is the smallest at 105 °. As such, 97.5 °, 105 ° and 112.5 ° are selected as the factor levels of the orthogonal test. The pipe diameter is negatively correlated with the erosion rate and the reduction rate decreases after 130 mm. 120 mm, 130 mm, and 140 mm are selected as the factor levels of the orthogonal test.

Orthogonal test and result analysis

Without considering the interaction of factors, $L_9(3^4)$ orthogonal test is designed to study the effect of test factors such as wind velocity (A), bending angle (B), and diameter of pipeline (C) on the erosion rate.

To obtain the optimal combination of pipeline structural optimization parameters through the polar analysis of data obtained from orthogonal test. The factor level coding of the orthogonal test is shown in Table 6.

Table 6

Experimental factors and corresponding level coding

Level	Considerations			
	Air velocity A (m·s-1)	Bend angle B (°)	Pipe Diameter C (mm)	Blank column
1	28	97.5	120	1
2	33	105	130	2
3	38	112.5	140	3

The orthogonal test results and polar analysis is shown in Table 7. The greater the polar difference between the factors, the greater the impact of the factors on the error. The polar analysis shows that the impact extent of factors on the erosion rate is: wind velocity > bending angle>pipe diameter. The smaller the erosion rate of the test indexes, the more in line with the actual working needs. Therefore, the optimal test combination is the smallest K value of each factor, and then A1B2C2 is the optimal test combination. Since the table does not include the group of tests, the combination of tests is verified that the erosion rate is 2.33E-7, which is the lowest in the 10 groups of tests. The optimal parameter combination is obtained as a wind velocity of 28 $m \cdot s^{-1}$, a bending angle of 105 °, and a pipe diameter of 130 mm.

Table 7

Orthogonal test results and extreme variance analysis

Serial number	Factor A	Factor B	Factor C	Blank column	Erosion rates
1	1	1	1	1	3.72E-07
2	1	2	3	2	2.48E-07
3	1	3	2	3	3.24E-07
4	2	1	3	3	4.05E-07
5	2	2	2	1	3.40E-07
6	2	3	1	2	5.64E-07
7	3	1	2	2	6.96E-07
8	3	2	1	3	6.27E-07
9	3	3	3	1	7.22E-07
K1	9.44E-07	1.47E-06	1.56E-06	1.43E-06	
K2	1.31E-06	1.22E-06	1.36E-06	1.51E-06	
K3	2.05E-06	1.61E-06	1.38E-06	1.36E-06	
k1	3.15E-07	4.91E-07	5.21E-07	4.78E-07	
k2	4.36E-07	4.05E-07	4.53E-07	5.03E-07	
k3	6.82E-07	5.37E-07	4.58E-07	4.52E-07	
Extremely poor	1.11E-06	3.95E-07	2.03E-07		
Optimal solution	A1	B2	C2		

Simulation of optimized pipeline

The optimal piping parameters are couple and simulated and remaining parameters are unchanged. The number of collisions and energy losses are as shown in Table 8.

Table 8

Coupling test results of the optimized pipe

Norm	Number of collisions			Energy loss		
	Pre-optimization	Post-optimization	Degree of optimization	Pre-optimi-zation	Post-optimization	Degree of optimization
Between jujubes	2330	1461	37.3%	14.83	12.77	13.87%
Between jujube and pipe wall	2688	2219	17.45%	24.45	20.14	17.61%

As shown in Table 8, the number of collisions and energy loss between jujubes after pipeline optimization are reduced by 37.3 % and 13.87 % year-on-year, respectively, and those between jujubes and pipe wall are reduced by 17.45 % and 17.61 % year-on-year, respectively. The reduction effect is obvious.

Test Verification for Optimized Pipeline

To test the feasibility of the simulation and optimization results of the conveying pipeline of the air suction jujube picker, it is verified through the test device. The test material was gray jujubes, and 500 red jujubes with intact skin were selected for test. Under the fixed wind velocity of 28 m/s of the conveying pipe, five tests were carried out on the un-optimized conveying pipeline and the optimized conveying pipeline respectively, so as to obtain the reduction values of jujube skin damage rate. After the completion of each group of tests, jujubes with cracked epidermis and exposed pulp were selected as epidermal damage, and the test results are shown in Table 9.

Table 9

Optimization test results

Test number	Reduction values of epidermal damage rate / %
1	2.2
2	1.8
3	2.6
4	1.6
5	2.1

According to the verification of the simulation test results by the test device, it can be seen that, the average epidermal damage rate of the pipeline after optimization is reduced by 2.06 %. This can reduce the damage of the pipe wall to the jujube epidermis to a certain extent, indicating that the optimized pipeline design is feasible.

CONCLUSIONS

(1) The CFD-DEM coupling method is used to simulate the movement process of jujube particles in the conveying pipeline, and the pipeline pressure, airflow distribution and the movement state of jujube particles in different parts of the pipeline are analyzed. According to the statistics of the number of collisions and energy loss between jujubes, as well as between jujubes and pipeline, it is found that these two kinds of collisions have a certain impact on the performance of conveying pipeline. The number of collisions and the energy loss between jujube particles and pipeline is large, and the impact on the conveying performance is more significant.

(2) Taking the erosion rate as the performance evaluation index, the wind velocity, bending angle and pipe diameter as the test factors, a single-factor test is carried out to determine the influence degree of each factor on the erosion rate. The orthogonal test method is used to further study the influence degree of each factor on the erosion rate, and the results show that wind velocity>bending angle>pipe diameter. The optimal parameter combination of the pipeline is a wind velocity of 28 $m \cdot s^{-1}$, a bending angle of 105 °, and a pipeline diameter of 130 mm.

(3) The verification results show that the number of collisions and energy loss between jujubes of the optimized pipeline are reduced by 37.3 % and 13.87 % year-on-year, and those between jujube particles and pipe wall are reduced by 17.45 % and 17.61 % year-on-year, respectively. The simulation test results verify that the average skin damage rate of optimized pipeline is reduced by 2.06 %, confirming that the optimizing the pipeline structural parameters can reduce the jujube skin damage to a certain extent.

ACKNOWLEDGEMENTS

This work was financially Supported by Bingtuan Science and Technology Program (Grant No. 2021CB018), and the Master Talent Project of the Tarim University Presidents Fund (Grant No. TDZKSS202110) for supporting this research. The authors are grateful to anonymous reviewers for their comments.

REFERENCES

[1] Basu, S., Chakrabarty, A., Nag, S., Behera, K., Bandyopadhyay, B., Grima, A. P., Ghosh, P. (2021). Design modification of iron ore bearing transfer chute using discrete element method. *Engineering Computations*, Vol. 38, No. 9, pp. 3590-3607.

[2] Brandt, V., Grabowski, J., Jurtz, N., Kraume, M., Kruggel-Emden, H. (2023). A benchmarking study of different DEM coarse graining strategies. *Powder Technology*, Vol. 426, 118629.

[3] Carr, M. J., Roessler, T., Robinson, P.W., Otto, H., Richter, C., Katterfeld, A., Wheeler, C. A. (2023). Calibration procedure of Discrete Element Method (DEM) parameters for wet and sticky bulk materials. *Powder Technology*, Vol. 429, 118919.

[4] Du, X.H., Han, C.J., Sheng, J.J., Diao, H.W., Song, D.l., Zhang, S.X. (2022). Optimized design and test of jujube picker（红枣捡拾机优化设计与试验）. *Chinese Journal of Agricultural Mechanical Chemistry*, Vol. 43, pp.43-50. (in Chinese)

[5] Dustin, S.W., Sanja, M. (2023). An Analysis of CFD-DEM with Coarse Graining for Turbulent Particle-Laden Jet Flows. *Fluids*, Vol. 8(7), 215.

[6] El-Emam, M. A., Zhou, L., Shi, W., Han, C. (2021). Performance evaluation of standard cyclone separators by using CFD–DEM simulation with realistic bio-particulate matter. *Powder Technology*, Vol. 385, pp. 374-394.

[7] Hamed, H., Behrad E., Reza. Z., Rahmat S.G., Navid, M. (2023). Comparative CFD-DEM study of flow regimes in spout-fluid beds. *Particuology*, Vol. 85, pp. 323-334.

[8] Hesse, R., Lösch, P., Antonyuk, S. (2023). CFD-DEM analysis of internal packing structure and pressure characteristics in compressible filter cakes using a novel elastic–plastic contact model. *Advanced Powder Technology*. Vol. 34, 104062.

[9] Hou, J.L., Ma D.X., Li H., Zhang Z.L., Zhou J.L., Shi, S. (2023). Design and experiments of a pneumatic centrifugal combined precision seed metering device for wheat (气力离心组合式小麦精量排种器设计与试验). *Journal of Agricultural Machinery*,
Available online: https://kns.cnki.net/kcms/detail/11.1964.S.20230731.1034.002.html (in Chinese)

[10] Hu, K., Dai, Y., Wang, Y. (2020). Research status and development trend of pneumatic direct seeding device for rice and oil (稻油兼用型气力式直播排种装置研究现状和发展趋势). *Agricultural Engineering*, Vol. 10(10), pp.8-11. (in Chinese)

[11] Jayasundara, C. T., Zhu, H. P. (2022). Impact energy of particles in ball mills based on DEM simulations and data-driven approach. *Powder Technology*, Vol. 395, pp. 226-234.

[12] Kim, J., Chung, M.Y. (2019) CFD-DEM Simulation of the Fluidized-bed Granulation of Food Powders. *Biotechnology and Bioprocess Engineering*, Vol. 24(1), pp. 569-578.

[13] Leno, G., Ying, C., Hubert, L. (2023). Coupled CFD-DEM Simulation of Seed Flow in Horizontal-Vertical Tube Transition. *Processes*, Vol. 11(3), pp. 909-909.

[14] Lewis, S., Antonia, B., Alberto, R.D., Mojtaba, G. (2022). Application of coarse-graining for large scale simulation of fluid and particle motion in spiral jet mill by CFD-DEM. *Powder Technology*, Vol. 411, 117926.

[15] Nijssen, T. M. J., Padding, J. T. J., Ottens, M. (2023). Hydrodynamics of expanded bed adsorption studied through CFD-DEM. *Chemical Engineering Science*, Vol. 280, 119027.

[16] Ponzini, R., Vià, R. D., Bnà, S., Cottini, C., Benassi, A. (2021). Coupled CFD-DEM model for dry powder inhalers simulation: Validation and sensitivity analysis for the main model parameters. *Powder Technology*, Vol. 385, pp. 119-226.

[17] Qin, M., Jin, Y., Luo, W., Wu, F., Shi, L.L., Gu, F.W., Cao, M.Z., Hu, Z.C. (2023). Measurement and CFD-DEM Simulation of Suspension Velocity of Peanut and Clay-Heavy Soil at Harvest Time. *Agronomy*, Vol. 13(7), 1735.

[18] Rakesh, K., Shibayan, S. (2023). Erosion analysis of radial flow hydraulic turbine components through FLUENT-EDEM coupling. *Powder Technology*, Vol. 428, 118800.

[19] Ren, D.Z., Yu, H.L., Zhang, R., Li, J.Q., Zhao, Y.B., Liu, F.B., Zhang, J.H., Wang, W. (2023). Measurement and CFD-DEM Simulation of Suspension Velocity of Peanut and Clay-Heavy Soil at Harvest Time. *Agronomy*, Vol. 12 (12), 2115.

[20] Shi, G.K., Li, J.B., Ding, L, P., Kan, Z. (2022a). Design and test of inertial airflow type jujube cleaning system（惯性气流式红枣清选系统设计与试验）. *Journal of Agricultural Machinery*, Vol. 53, pp.167-176.

[21] Shi, G.K., Li, J.B., Ding, L.P., Zhang, Z.Y., Ding, H.Z., Li, N., Kan, Z. (2022b). Calibration and Tests for the Discrete Element Simulation Parameters of Fallen Jujube Fruit. *Agriculture*, Vol.12, pp. 38.

[22] Wang, C.X. (2021). Experimental Study and Parameter Optimization of Comb-Brush Roller Type Picking Device of Ground Jujube; *Shihezi University*: Xinjiang, China.

[23] Weaver, S.D., Mišković, S. (2023). An Analysis of CFD-DEM with Coarse Graining for Turbulent Particle-Laden Jet Flows. *Fluids*, Vol. 8(7), pp. 215.

[24] Weng, X.X., Chen, C.Q., Wang, G., Wei, Z.B., Jiang, L., Hu, X.R. (2022). Numerical Simulation of Leaf Gathering Process of Fresh Leaf Collecting Pipeline Based on CFD-DEM (基于CFD-DEM的机采鲜叶管道集叶过程数值模拟研究). *Journal of Agricultural Machinery*, Vol. 53(11), pp. 424-432. (in Chinese)

[25] Wiacek, J. (2016). Geometrical parameters of binary granular mixtures with size ratio and volume fraction: experiments and DEM simulations. *Granular Matter*, Vol.18, pp. 42.

[26] Xiong, P. Y., Xue M.J., Wang Y., Zhang, H.X., Xue, X.Q., Li, Z.L., Hu, W.Q. (2019). Simulation analysis and test of air suction oil tea seed shell kernel cleaning device. *Journal of Zhongkai Agricultural Engineering College*, Vol. 32(01), pp. 35-40+45.

[27] Yuan, P.P., Li S.F., Han C.J., Zhang, J., Xu Y. (2021). Design and test of hydraulic system of sweeping-air suction type date picker（清扫—气吸式红枣捡拾机液压系统设计与试验）. *China Agricultural Machinery Chemical Journal*, Vol. 42, pp. 28-33. (in Chinese)

[28] Yuan, Y.W., Bai, S.H., Niu K., Zhou, L.M., Zhao, B., Wei, L.G., Xiong, S., Liu, L.J. (2022). Advances in mechanized harvesting technology and equipment for forest and fruit（林果机械化采收技术与装备研究进展）. *Journal of Agricultural Engineering*, Vol. 38, pp. 53-63.

[29] Zhang, F.K., Ran, J.H., Li, Z.J., Wang, D.W., Li, P. (2021). Air-suction landing jujube picker operating parameters optimization（气吸式落地红枣捡拾机作业参数优化）. *Fruit Tree Journal*, Vol. 38, pp. 1190-1200. (in Chinese)

[30] Zhang, F.K., Yu, F.F., Li, Z.J., Zhang, H., Lan, H.P., Li, P., Zhang, C.J. (2020). Design and experiment of air-suction landing jujube picker（气吸式落地红枣捡拾机的设计与试验）. *Acta Pomologya Sinica*, Vol. 37, pp. 278-285. (in Chinese)

[31] Zhang, T., Liu, F., Zhao, M.Q., Ma. Q., Wang, W., Fan, Q., Yan, P. (2018). Determination of physical parameters of corn stover contact with discrete element simulation calibration（玉米秸秆接触物理参数测定与离散元仿真标定）. *Journal of China Agricultural University*, Vol. 4, pp.120-127. (in Chinese)

[32] Zhang, X.J., Bai, S.H., Jin W., Yuan, P.P., Yu, M.J., Yan, J.S., Zhang, C.S. (2019). Development of pneumatic pick-up machine for low density cultivation of jujubes（气力式矮密栽培红枣捡拾机研制）. *Journal of Agricultural Engineering*, Vol. 35, pp.1-9. (in Chinese)